
Improving GFlowNets with Monte Carlo Tree Search

Nikita Morozov^{1,2} Daniil Tiapkin^{3,4} Sergey Samsonov¹ Alexey Naumov^{1,5} Dmitry Vetrov⁶

Abstract

Generative Flow Networks (GFlowNets) treat sampling from distributions over compositional discrete spaces as a sequential decision-making problem, training a stochastic policy to construct objects step by step. Recent studies have revealed strong connections between GFlowNets and entropy-regularized reinforcement learning. Building on these insights, we propose to enhance planning capabilities of GFlowNets by applying Monte Carlo Tree Search (MCTS). Specifically, we show how the MENTS algorithm (Xiao et al., 2019) can be adapted for GFlowNets and used during both training and inference. Our experiments demonstrate that this approach improves the sample efficiency of GFlowNet training and the generation fidelity of pre-trained GFlowNet models.

1. Introduction

Generative Flow Networks (GFlowNets, Bengio et al., 2021) are models designed to sample compositional discrete objects, such as graphs, from distributions defined by unnormalized probability mass functions. They achieve this by training a stochastic policy to generate objects through a sequence of constructive actions to match the desired distribution. GFlowNets have been successfully applied in various areas, including biological sequence design (Jain et al., 2022), large language model (LLM) fine-tuning (Hu et al., 2023), combinatorial optimization (Zhang et al., 2023), neural architecture search (Chen & Mauch, 2023), and causal discovery (Atanackovic et al., 2024).

GFlowNets incorporate many concepts and techniques from reinforcement learning (RL). Recent works (Tiapkin et al.,

2024; Mohammadpour et al., 2024; Deleu et al., 2024) have shown that the GFlowNet learning problem can be reformulated as an RL problem with entropy regularization (Neu et al., 2017; Geist et al., 2019). These findings opened a direct way to apply many existing RL algorithms (Schulman et al., 2017; Haarnoja et al., 2017; 2018) to GFlowNets, and our work follows this path.

Monte Carlo Tree Search (MCTS) is a well-known method for solving planning problems (Coulom, 2006; Kocsis & Szepesvári, 2006). Prominent examples of RL algorithms utilizing MCTS include AlphaGo (Silver et al., 2016) and AlphaZero (Silver et al., 2018), which combine MCTS with deep neural networks to achieve super-human performance in games like Go, chess, and Shogi. MCTS algorithms typically require knowledge of the environment’s underlying dynamics or can be paired with a neural network-based simulator, as seen in MuZero-type approaches (Schrittwieser et al., 2020), resulting in a complicated algorithm. Fortunately, GFlowNets fall into the first category because the directed acyclic graph (DAG) environments they operate in are integral to the algorithm’s design and, moreover, deterministic. Thus, *the ability to simulate any trajectory in a deterministic DAG environment makes the idea of enhancing the planning abilities of GFlowNets with MCTS very natural.*

We focus on the Maximum Entropy for Tree Search (MENTS, Xiao et al., 2019) algorithm, an MCTS algorithm that estimates entropy-regularized Q-values. This entropy-regularized nature of this algorithm allows it to be directly applied to the framework of GFlowNets. **We outline our contributions as follows:** *i)* We show how MENTS coupled with SoftDQN (Haarnoja et al., 2017) can be applied to GFlowNets at both training and inference stages, *ii)* we experimentally demonstrate how improved planning capabilities can benefit GFlowNets.

2. Background

2.1. GFlowNets

Suppose we have a finite space \mathcal{X} and a black-box non-negative function $R: \mathcal{X} \rightarrow \mathbb{R}_{\geq 0}$, which we will call the *GFlowNet reward*. Our goal is to sample objects from \mathcal{X} with probabilities $R(x)/Z$, where $Z = \sum_{x \in \mathcal{X}} R(x)$ is an unknown normalizing constant.

arXiv:2406.13655v1 [cs.LG] 19 Jun 2024

¹HSE University, Moscow, Russia ²Skoltech, Moscow, Russia
³CMAP – CNRS – École polytechnique – Institut Polytechnique de Paris, 91128, Palaiseau, France ⁴Université Paris-Saclay, CNRS, LMO, 91405, Orsay, France ⁵Steklov Mathematical Institute of Russian Academy of Sciences ⁶Constructor University, Bremen. Correspondence to: Nikita Morozov <nmorozov@hse.ru>.

Accepted by the Structured Probabilistic Inference & Generative Modeling workshop of ICML 2024, Vienna, Austria. Copyright 2024 by the author(s).

Consider a finite directed acyclic graph (DAG) $\mathcal{G} = (\mathcal{S}, \mathcal{E})$, where \mathcal{S} is a state space and $\mathcal{E} \subseteq \mathcal{S} \times \mathcal{S}$ is a set of edges. Non-terminal states correspond to "incomplete" objects, with an empty object denoted as s_0 , and edges represent adding new components to these objects. Every state can be reached from s_0 , which has no incoming edges. Terminal states are "complete" objects and coincide with \mathcal{X} . Let \mathcal{T} denote the set of all complete trajectories $\tau = (s_0 \rightarrow s_1 \rightarrow \dots \rightarrow s_{n_\tau})$ in the graph, where τ is a sequence of transitions $s_i \rightarrow s_{i+1} \in \mathcal{E}$ from s_0 to some terminal state $s_{n_\tau} \in \mathcal{X}$.

Next, we introduce probability distributions over the children of each state $P_F(s_t | s_{t-1})$ and the parents of each state $P_B(s_{t-1} | s_t)$, called the *forward policy* and the *backward policy*, respectively. The main goal is to find a pair of policies such that the induced distributions over complete trajectories in the forward and backward directions coincide:

$$\prod_{t=1}^{n_\tau} P_F(s_t | s_{t-1}) = \frac{R(s_{n_\tau})}{Z} \prod_{t=1}^{n_\tau} P_B(s_{t-1} | s_t) \quad \forall \tau \in \mathcal{T}. \quad (1)$$

This is known as the *trajectory balance constraint* (Malkin et al., 2022). If this constraint is satisfied for all complete trajectories, sampling a trajectory in the forward direction using P_F will result in a terminal state being sampled with probability $R(x)/Z$.

In practice, GFlowNet is a model that parameterizes the forward policy (and possibly other components) trained to minimize an objective function that enforces the constraint (1) or an equivalent one. Among existing training objectives, *Subtrajectory Balance* (SubTB, Madan et al., 2023) has been shown experimentally to have superior performance across various tasks. Notably, the backward policy can either be trained alongside the forward policy or fixed, for example, to be uniform over the parents of each state. For any fixed backward policy, there exists a unique forward policy that satisfies (1) (Malkin et al., 2022). For further details on GFlowNets, we refer to (Bengio et al., 2023).

2.2. GFlowNets as Soft RL

In contrast to the classical RL formulation of reward maximization, entropy-regularized RL (Neu et al. 2017; Geist et al. 2019; Haarnoja et al. 2017, also known as soft RL) augments the value function by Shannon entropy \mathcal{H} :

$$V_\lambda^\pi(s) \triangleq \mathbb{E}_\pi \left[\sum_{t=0}^{\infty} \gamma^t (r(s_t, a_t) + \lambda \mathcal{H}(\pi(s_t))) | s_0 = s \right], \quad (2)$$

where λ is a regularization coefficient. Similarly, we can define regularized Q-values $Q_\lambda^\pi(s, a)$ as an expected (discounted) sum of rewards augmented by Shannon entropy given a fixed initial state $s_0 = s$ and action $a_0 = a$. A regularized optimal policy π_λ^* is a policy that maximizes $V_\lambda^\pi(s)$ for any initial state s .

Let V_λ^* and Q_λ^* be the value and the Q-value of the optimal policy π_λ^* correspondingly. Then Theorem 1 and 2 by (Haarnoja et al., 2017) imply the following system relations for any state-action pair s, a for a deterministic environment

$$Q_\lambda^*(s, a) = r(s, a) + \gamma \text{LSE}_\lambda(Q_\lambda^*(s', \cdot)), \quad (3)$$

where s' is a next state after taking an action a in a state s , $\text{LSE}_\lambda(Q(s', \cdot)) \triangleq \lambda \log(\sum_{a'} \exp\{Q(s', a')/\lambda\})$. Then the optimal policy can be computed as $\pi_\lambda^*(\cdot | s) \triangleq \text{Softmax}(Q_\lambda^*(s, \cdot)/\lambda)$.

(Tiapkin et al., 2024) showed that the problem of GFlowNet forward policy training given a fixed backward policy can be equivalently formulated as an entropy-regularized RL problem. This reduction involves adding an absorbing state s_f to the GFlowNet DAG, with edges from terminal states to s_f and a loop $s_f \rightarrow s_f$. A deterministic Markov Decision Process (MDP) is then constructed from the DAG, where states correspond to DAG states and actions correspond to edges (or, equivalently, to next possible states). RL rewards are set for all edges as follows:

$$r(s, s') \triangleq \begin{cases} \log P_B(s | s') & s \notin \mathcal{X} \cup \{s_f\}, \\ \log R(s) & s \in \mathcal{X}, \\ 0 & s = s_f. \end{cases} \quad (4)$$

Theorem 1 of (Tiapkin et al., 2024) states that the optimal policy $\pi_1^*(s' | s)$ in this MDP, with λ set to 1 and $\gamma = 1$, coincides with the GFlowNet forward policy P_F (which is uniquely defined by P_B and R).

This reduction enables the direct application of soft RL algorithms to GFlowNet training. (Tiapkin et al., 2024) applied the classical `SOFTDQN` algorithm (Haarnoja et al., 2017) and demonstrated its efficiency. Essentially, a neural network is trained to predict optimal regularized Q-values for all transitions using the following objective:

$$(Q_\theta(s, s') - \log P_B(s | s') - \text{LSE}(Q_{\bar{\theta}}(s', \cdot)))^2, \quad (5)$$

where $\text{LSE}(Q_{\bar{\theta}}(s', \cdot)) \triangleq \text{LSE}_1(Q_{\bar{\theta}}(s', \cdot))$ is replaced with $\log R(s')$ if $s' \in \mathcal{X}$, and $\bar{\theta}$ are parameters of a target network that is updated with weights θ from time to time. The corresponding policy is computed as $\pi_\theta(\cdot | s) = \text{Softmax}(Q_\theta(s, \cdot))$. The model can be either trained on-policy by optimizing the loss over complete trajectories sampled from π_θ or utilize a replay buffer.

3. Method

In RL planning, the agent needs to determine the optimal action to maximize future rewards in a large state space. The simplest method is to train a Q-network to predict the expected future rewards for each action and choose the

one with the highest predicted Q-value. However, this approach depends heavily on the Q-network’s approximation capabilities and may not fully leverage the problem’s structure. In contrast, MCTS algorithms look multiple steps ahead to evaluate the future state of the environment better. MCTS incrementally builds a look-ahead tree, balancing the exploration-exploitation trade-off during navigation in the tree (Kocsis & Szepesvári, 2006). Each new node added to the tree is evaluated either through a Monte Carlo simulation or neural network prediction, and this information is backpropagated along the path to the root.

In GFlowNets, the planning problem differs because we need to determine not just a single optimal action but the optimal distribution over possible actions (forward policy). This can be achieved by training a Q-network, as the optimal policy is the softmax of optimal entropy-regularized Q-values. However, using look-ahead information from MCTS can provide better estimates of Q-values in a similar fashion to the RL setting. Therefore, we propose a direct adaptation of the MENTS algorithm (Xiao et al., 2019), which aims to improve the estimation of optimal entropy-regularized Q-values. Below, we describe how MENTS can be applied to GFlowNet inference and training on top of `SOFTDQN`, following the paradigm described in Section 2.2.

3.1. MENTS for GFlowNets

Inference stage. Suppose we have a pre-trained neural network Q_θ that predicts soft Q-values. The root of the look-ahead tree corresponds to the current DAG state s_{root} . For each node of the tree, we store a visit count $N(s)$, and for each edge $s \rightarrow s'$, we store an estimate $Q_{\text{tree}}(s, s')$ of the regularized Q-value.

During each round of MCTS, we sample a path from the root to some leaf of the tree by sequentially sampling a child from the tree policy, that is, a softmax policy with respect to Q_{tree} with an additional ε -greedy exploration:

$$\pi_{\text{tree}}(\cdot | s) = (1-p_s)\text{Softmax}(Q_{\text{tree}}(s, \cdot)) + p_s \cdot \mathcal{U}(C(s)), \quad (6)$$

where $\mathcal{U}(C(s))$ is a uniform distribution over the children of s denoted by $C(s)$, and $p_s = \varepsilon |C(s)| / \log(N(s) + 2)$, where ε is an exploration hyperparameter.

Let (s_1, s_2, \dots, s_T) be the sampled path, where $s_1 = s_{\text{root}}$ and s_T is a leaf. Then, we add new nodes and edges to the tree corresponding to the children of s_T in the GFlowNet DAG \mathcal{G} . For each added child $s' \in C(s_T)$, we initialize $N(s') = 0$ and $Q_{\text{tree}}(s_T, s') = Q_\theta(s_T, s')$. Then, for each node in the path, we update $N(s_i) = N(s_i) + 1$, and for each edge in the path from last to first, we update the Q-value estimate, following the optimality condition (3)

$$Q_{\text{tree}}(s_i, s_{i+1}) = \log P_B(s_i | s_{i+1}) + \text{LSE}(Q_{\text{tree}}(s_{i+1}, \cdot)). \quad (7)$$

A special case arises when s_T is a terminal state of \mathcal{G} . No nodes will be added to the tree in this case, and as for updating $Q_{\text{tree}}(s_{T-1}, s_T)$, there are two options. The first option is to replace $\text{LSE}(Q_{\text{tree}}(s_T, \cdot))$ with $\log R(s_T)$ (since $\log R(s_T)$ coincides with $V_1^*(s_T)$, see Tiapkin et al., 2024). However, in potential scenarios with no access to GFlowNet reward R during inference or its calculation being very expensive (e.g., drug discovery, see Jain et al., 2023), this option may not be very practical. The second option is to skip the update of $Q_{\text{tree}}(s_{T-1}, s_T)$, leaving it as it was initialized by $Q_\theta(s_{T-1}, s_T)$. Then the algorithm only requires access to Q_θ , $\log P_B$, and the structure of \mathcal{G} , making it applicable in all practical cases. All experiments in Section 4 are carried out with this option.

After all rounds of MCTS, we have an estimate $Q_{\text{tree}}(s_{\text{root}}, s')$ for each child s' of the root, and the resulting forward policy can be obtained as $\text{Softmax}(Q_{\text{tree}}(s_{\text{root}}, \cdot))$. The next state is sampled from this policy, and the tree’s root is changed to the corresponding child, possibly already having a non-empty subtree. Note that the number of times Q_θ is evaluated is upper bounded by the number of MCTS rounds (assuming Q_θ takes a state as an input and outputs predictions for all possible actions). In practice, we fix the maximum visit count of the root $N(s_{\text{root}})$ as a hyperparameter; thus, the number of rounds can vary depending on the number of visits to the state before it becomes the root.

An important point is that the presented algorithm does not require \mathcal{G} itself to be a tree and can work in arbitrary GFlowNet environments. If a state in \mathcal{G} is reached by a number of different paths during MCTS, there will be multiple nodes in the tree corresponding to the same state. Appendix A presents a detailed pseudocode of the algorithm and its connection to GFlowNet flow functions.

Training stage. Consider `SOFTDQN` training objective (5). It can be viewed as fitting $Q_\theta(s, s')$ on a one-step MENTS estimate calculated using the current target network $Q_{\bar{\theta}}$. However, one can run multiple rounds of MCTS to obtain better targets for fitting the Q-network, which allows us to utilize MCTS for training Q_θ . The training objective becomes

$$(Q_\theta(s, s') - Q_{\text{tree}}(s, s'))^2, \quad (8)$$

where $Q_{\text{tree}}(s, s')$ is obtained by applying MENTS with the current target network $Q_{\bar{\theta}}$ instead of a fixed pre-trained one. Since we do not provide access to GFlowNet rewards during MCTS, an exception is a loss for transitions into terminal states $s' \in \mathcal{X}$, which we take to be

$$(Q_\theta(s, s') - \log P_B(s | s') - \log R(s'))^2. \quad (9)$$

Such a choice also allows for a more straightforward comparison with other methods in terms of the number of calls to $R(x)$ made during training.

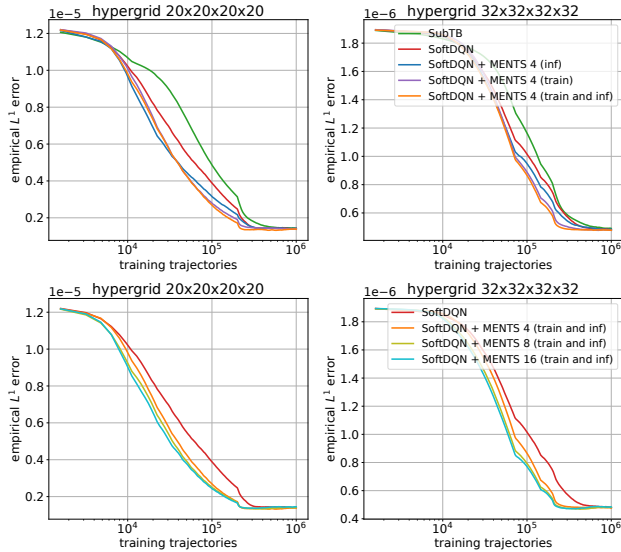


Figure 1. L^1 distance between target and empirical sample distributions over the course of training on the hypergrid environment. Numbers next to MENTS in the legend correspond to maximum number of MCTS rounds $N(s_{\text{root}})$.

4. Experiments

We carry out experimental evaluation on hypergrid (Bengio et al., 2021) and bit sequence (Malkin et al., 2022) environments following similar experimental setups to (Tiapkin et al., 2024). Along with SoftDQN and MENTS, we provide SubTB (Madan et al., 2023) as a baseline. In all experiments, P_B is fixed to be uniform. Appendix B contains additional experimental details and runtime measurements for the compared algorithms.

4.1. Hypergrid Environment

The set of states corresponds to two copies of points (non-terminal and terminal) with integer coordinates inside a 4-dimensional hypercube with side length H . The allowed actions are to increase on coordinate by 1 without exiting the grid and to move to a terminal copy of the state. Initial state s_0 is $(0, 0, 0, 0)$. The reward has modes near the corners of the grid, separated by wide troughs with a very small reward. All models are parameterized by MLP with one-hot encoded inputs.

We study 3 setups: 1) a model is trained with vanilla SoftDQN and evaluated with MENTS; 2) a model is trained with MENTS targets, but the trained policy is evaluated without MCTS; 3) MENTS is applied for both training and evaluation. In contrast to (Tiapkin et al., 2024), we do not use replay buffers for training, instead optimizing the loss across trajectories sampled from the current model. As a metric we use L^1 distance between the true reward distribution $R(x)/Z$ (Z can be computed exactly since environments are

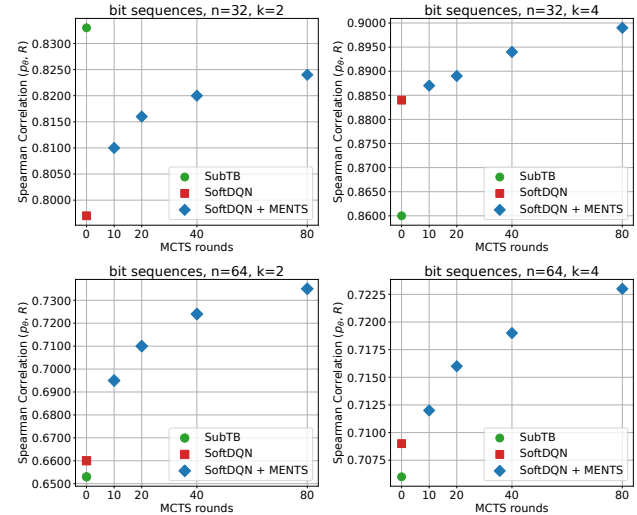


Figure 2. Spearman correlation between R and P_θ on a test set for varying n and k in the bit sequence generation task. MENTS is used here only at the inference stage.

small) and an empirical distribution of $2 \cdot 10^5$ GFlowNet samples.

Figure 1 presents the results. We can see that in all setups MENTS offers a stable improvement to the speed of convergence in comparison to vanilla SoftDQN in terms of number of sampled trajectories, which coincides with the number of calls to $R(x)$. The best results are obtained when MENTS is applied for both training and inference of the model. Remarkably, using MENTS to compute targets for the training of Q_θ provides a noticeable boost even when the model is evaluated without MCTS (setup number 2). Increasing the number of MCTS rounds is also beneficial.

4.2. Bit Sequence Generation

The goal is to generate binary strings of some fixed length n . Hyperparameter $k \mid n$ is introduced, and the string is split into n/k segments of length k . Each state corresponds to a sequence of n/k words; each word is either an empty word \emptyset or one of 2^k possible k -bit words. s_0 corresponds to a sequence of empty words. Possible actions are to take any position with an empty word and replace it with any k -bit word. Terminal states contain no empty words and coincide with binary strings of length n . $R(x) = \exp(-2 \cdot \min_{x' \in M} d(x, x'))$, where M is a set of modes and d is Hamming distance. We use this environment to examine the performance of MCTS in a more challenging setup with larger state and action spaces (up to $\approx 2 \cdot 10^{22}$ states and 256 actions in our experiments).

Here we train Q_θ with SoftDQN parameterized by Transformer (Vaswani et al., 2017) and utilize MENTS *only during inference*. Following (Tiapkin et al., 2024) we compute

Spearman correlation on a test set of strings between R and an estimate of sampling probability P_θ . The results are presented in Figure 2. In all configurations, enhancing SoftDQN with MENTS improves the reward correlation in comparison to vanilla SoftDQN, although the improvement is relatively small in some cases. It also outperforms SubTB in 3 out of 4 cases. The metric steadily rises with the increase of the number of MCTS rounds.

5. Conclusion

In this paper, we proposed to apply MENTS (Xiao et al., 2019) algorithm with SoftDQN (Haarnoja et al., 2017) to GFlowNet training and inference. Our experimental results demonstrated the benefits of incorporating MCTS planning for amortized sampling, suggesting new research directions. Future work could explore other MCTS-type approaches, validate them in other domains, and apply MCTS on top of other GFlowNet algorithms, e.g. SubTB (Madan et al., 2023).

Acknowledgements

The work of Nikita Morozov, Sergey Samsonov and Alexey Naumov was supported by the grant for research centers in the field of AI provided by the Analytical Center for the Government of the Russian Federation (ACRF) in accordance with the agreement on the provision of subsidies (identifier of the agreement 000000D730321P5Q0002) and the agreement with HSE University No. 70-2021-00139. The work of Daniil Tiapkin was supported by the Paris Île-de-France Région in the framework of DIM AI4IDF. This research was supported in part through computational resources of HPC facilities at HSE University (Kostenetskiy et al., 2021).

References

- Atanackovic, L., Tong, A., Wang, B., Lee, L. J., Bengio, Y., and Hartford, J. S. Dyngfn: Towards bayesian inference of gene regulatory networks with gflownets. *Advances in Neural Information Processing Systems*, 36, 2024.
- Bengio, E., Jain, M., Korablyov, M., Precup, D., and Bengio, Y. Flow network based generative models for non-iterative diverse candidate generation. *Advances in Neural Information Processing Systems*, 34:27381–27394, 2021.
- Bengio, Y., Lahlou, S., Deleu, T., Hu, E. J., Tiwari, M., and Bengio, E. Gflownet foundations. *Journal of Machine Learning Research*, 24(210):1–55, 2023.
- Chen, Y. and Mauch, L. Order-preserving gflownets. In *The Twelfth International Conference on Learning Representations*, 2023.
- Coulom, R. Efficient selectivity and backup operators in monte-carlo tree search. In *International conference on computers and games*, pp. 72–83. Springer, 2006.
- Deleu, T., Nouri, P., Malkin, N., Precup, D., and Bengio, Y. Discrete probabilistic inference as control in multi-path environments. *arXiv preprint arXiv:2402.10309*, 2024.
- Geist, M., Scherrer, B., and Pietquin, O. A theory of regularized markov decision processes. In *International Conference on Machine Learning*, pp. 2160–2169. PMLR, 2019.
- Haarnoja, T., Tang, H., Abbeel, P., and Levine, S. Reinforcement learning with deep energy-based policies. In *International conference on machine learning*, pp. 1352–1361. PMLR, 2017.
- Haarnoja, T., Zhou, A., Abbeel, P., and Levine, S. Soft actor-critic: Off-policy maximum entropy deep reinforcement learning with a stochastic actor. In *International conference on machine learning*, pp. 1861–1870. PMLR, 2018.
- Hu, E. J., Jain, M., Elmoznino, E., Kaddar, Y., Lajoie, G., Bengio, Y., and Malkin, N. Amortizing intractable inference in large language models. In *The Twelfth International Conference on Learning Representations*, 2023.
- Jain, M., Bengio, E., Hernandez-Garcia, A., Rector-Brooks, J., Dossou, B. F., Ekbote, C. A., Fu, J., Zhang, T., Kilgour, M., Zhang, D., et al. Biological sequence design with gflownets. In *International Conference on Machine Learning*, pp. 9786–9801. PMLR, 2022.
- Jain, M., Deleu, T., Hartford, J., Liu, C.-H., Hernandez-Garcia, A., and Bengio, Y. Gflownets for ai-driven scientific discovery. *Digital Discovery*, 2(3):557–577, 2023.
- Kocsis, L. and Szepesvári, C. Bandit based monte-carlo planning. In *European conference on machine learning*, pp. 282–293. Springer, 2006.
- Kostenetskiy, P., Chulkevich, R., and Kozyrev, V. Hpc resources of the higher school of economics. In *Journal of Physics: Conference Series*, volume 1740, pp. 012050. IOP Publishing, 2021.
- Madan, K., Rector-Brooks, J., Korablyov, M., Bengio, E., Jain, M., Nica, A. C., Bosc, T., Bengio, Y., and Malkin, N. Learning gflownets from partial episodes for improved convergence and stability. In *International Conference on Machine Learning*, pp. 23467–23483. PMLR, 2023.
- Malkin, N., Jain, M., Bengio, E., Sun, C., and Bengio, Y. Trajectory balance: Improved credit assignment in gflownets. *Advances in Neural Information Processing Systems*, 35:5955–5967, 2022.

- Mnih, V., Kavukcuoglu, K., Silver, D., Rusu, A. A., Veness, J., Bellemare, M. G., Graves, A., Riedmiller, M., Fidjeland, A. K., Ostrovski, G., et al. Human-level control through deep reinforcement learning. *nature*, 518(7540): 529–533, 2015.
- Mohammadpour, S., Bengio, E., Frejinger, E., and Bacon, P.-L. Maximum entropy gflownets with soft q-learning. In *International Conference on Artificial Intelligence and Statistics*, pp. 2593–2601. PMLR, 2024.
- Neu, G., Jonsson, A., and Gómez, V. A unified view of entropy-regularized markov decision processes. *arXiv preprint arXiv:1705.07798*, 2017.
- Paszke, A., Gross, S., Massa, F., Lerer, A., Bradbury, J., Chanan, G., Killeen, T., Lin, Z., Gimelshein, N., Antiga, L., et al. Pytorch: An imperative style, high-performance deep learning library. *Advances in neural information processing systems*, 32, 2019.
- Schaul, T., Quan, J., Antonoglou, I., and Silver, D. Prioritized experience replay. In Bengio, Y. and LeCun, Y. (eds.), *4th International Conference on Learning Representations, ICLR 2016, San Juan, Puerto Rico, May 2-4, 2016, Conference Track Proceedings*, 2016. URL <http://arxiv.org/abs/1511.05952>.
- Schrittwieser, J., Antonoglou, I., Hubert, T., Simonyan, K., Sifre, L., Schmitt, S., Guez, A., Lockhart, E., Hassabis, D., Graepel, T., et al. Mastering atari, go, chess and shogi by planning with a learned model. *Nature*, 588(7839): 604–609, 2020.
- Schulman, J., Chen, X., and Abbeel, P. Equivalence between policy gradients and soft q-learning. *arXiv preprint arXiv:1704.06440*, 2017.
- Silver, D., Huang, A., Maddison, C. J., Guez, A., Sifre, L., Van Den Driessche, G., Schrittwieser, J., Antonoglou, I., Panneershelvam, V., Lanctot, M., et al. Mastering the game of go with deep neural networks and tree search. *nature*, 529(7587):484–489, 2016.
- Silver, D., Hubert, T., Schrittwieser, J., Antonoglou, I., Lai, M., Guez, A., Lanctot, M., Sifre, L., Kumaran, D., Graepel, T., Lillicrap, T., Simonyan, K., and Hassabis, D. A general reinforcement learning algorithm that masters chess, shogi, and go through self-play. *Science*, 362(6419):1140–1144, 2018. doi: 10.1126/science.aar6404.
- Tiapkin, D., Morozov, N., Naumov, A., and Vetrov, D. P. Generative flow networks as entropy-regularized rl. In *International Conference on Artificial Intelligence and Statistics*, pp. 4213–4221. PMLR, 2024.
- Vaswani, A., Shazeer, N., Parmar, N., Uszkoreit, J., Jones, L., Gomez, A. N., Kaiser, Ł., and Polosukhin, I. Attention is all you need. *Advances in neural information processing systems*, 30, 2017.
- Xiao, C., Huang, R., Mei, J., Schuurmans, D., and Müller, M. Maximum entropy monte-carlo planning. *Advances in Neural Information Processing Systems*, 32, 2019.
- Zhang, D., Dai, H., Malkin, N., Courville, A. C., Bengio, Y., and Pan, L. Let the flows tell: Solving graph combinatorial problems with gflownets. In *Advances in Neural Information Processing Systems*, volume 36, pp. 11952–11969, 2023.

A. Algorithm Details

Algorithm 1 presents a detailed pseudo-code for sampling a trajectory with MENTS applied on top of a GFlowNet pre-trained with SoftDQN.

Algorithm 1 Inference of SoftDQN + MENTS

```

1: Input: SoftDQN pre-trained  $Q_\theta$ , maximum number of MCTS rounds  $N_{\max}$ , exploration parameter  $\varepsilon$ , GFlowNet
   backward policy  $P_B$ 
2: Initialize  $s_{\text{root}} = s_0$ ,  $N(s_{\text{root}}) = 0$ 
3: repeat
4:   while  $N(s_{\text{root}}) < N_{\max}$  do
5:     Initialize  $\text{path} = \{s_{\text{root}}\}$ 
6:     while  $\text{path.last}$  is not a leaf do
7:       Initialize  $s = \text{path.last}$ 
8:       Compute  $p_s = \varepsilon |C(s)| / \log(N(s) + 2)$ 
9:       Compute  $\pi_{\text{tree}}(\cdot | s) = (1 - p_s) \cdot \text{Softmax}(Q_{\text{tree}}(s, \cdot)) + p_s \cdot \mathcal{U}(C(s))$ 
10:      Sample  $s' \sim \pi_{\text{tree}}(\cdot | s)$ 
11:      Append  $s'$  to  $\text{path}$ 
12:      Update  $N(s') = N(s') + 1$ 
13:    end while
14:    Initialize  $s_{\text{leaf}} = \text{path.last}$ 
15:    if  $s_{\text{leaf}} \notin \mathcal{X}$  then
16:      for all  $s' \in C(s_{\text{leaf}})$  do
17:        Add  $s'$  to the tree
18:        Initialize  $N(s') = 0$ 
19:        Initialize  $Q_{\text{tree}}(s_{\text{leaf}}, s') = Q_\theta(s_{\text{leaf}}, s')$ 
20:      end for
21:    end if
22:    for  $i = \text{path.size} - 1$  to 1 do
23:      if  $\text{path}_{i+1} \notin \mathcal{X}$  then
24:        Update  $Q_{\text{tree}}(\text{path}_i, \text{path}_{i+1}) = \log P_B(\text{path}_i | \text{path}_{i+1}) + \text{LSE}(Q_{\text{tree}}(\text{path}_{i+1}, \cdot))$ 
25:      end if
26:    end for
27:  end while
28:  Compute  $P_F(\cdot | s_{\text{root}}) = \text{Softmax}(Q_{\text{tree}}(s_{\text{root}}, \cdot))$ 
29:  Sample  $s_{\text{next}} \sim P_F(\cdot | s_{\text{root}})$ 
30:  Delete everything from the tree except the subtree of  $s_{\text{next}}$ 
31:  Update  $s_{\text{root}} = s_{\text{next}}$ 
32: until  $s_{\text{root}}$  corresponds to a terminal state  $x \in \mathcal{X}$ 
33: Output terminal state  $x$ 

```

A.1. Connection to GFlowNet State and Edge Flows

Suppose we have forward and backward policies that satisfy trajectory balance constraints (1). Then, we have a fixed distribution over complete trajectories

$$P(\tau) = \prod_{t=1}^{n_\tau} P_F(s_t | s_{t-1}) = \frac{R(s_{n_\tau})}{Z} \prod_{t=1}^{n_\tau} P_B(s_{t-1} | s_t). \quad (10)$$

GFlowNet literature often operates with *flows* functions (Bengio et al., 2023). *Markovian flow* in this case is a function $F: \mathcal{T} \rightarrow \mathbb{R}_{\geq 0}$ that coincides with unnormalized probability of sampling a trajectory $F(\tau) = Z \cdot P(\tau)$. Since for any fixed P_B and R there exists a unique P_F satisfying (1), any fixed P_B and R also define a unique Markovian flow. *State flows* and *edge flows* are defined as $F(s) = \sum_{\tau \ni s} F(\tau)$, $F(s \rightarrow s') = \sum_{\tau \ni (s \rightarrow s')} F(\tau)$ correspondingly, and coincide with unnormalized probabilities that a trajectory passes through some state/edge.

Flow matching constraint states that for any state that is not s_0 or terminal

$$F(s) = \sum_{s \rightarrow s'} F(s \rightarrow s') = \sum_{s'' \rightarrow s} F(s'' \rightarrow s), \quad (11)$$

while for s_0 and terminal states, only one of the two equalities holds.

P_F and P_B can be computed in terms of state and edge flows

$$P_F(s' | s) = \frac{F(s \rightarrow s')}{F(s)}, \quad P_B(s | s') = \frac{F(s \rightarrow s')}{F(s')}. \quad (12)$$

Let us go back to the RL interpretation. In addition to the optimal policy, Theorem 1 of (Tiapkin et al., 2024) connects state and edge flows with optimal entropy-regularized values and Q-values, stating

$$V_1^*(s) = \log F(s), \quad Q_1^*(s, s') = \log F(s \rightarrow s'). \quad (13)$$

In this interpretation, (3) transforms into

$$\begin{aligned} \log F(s \rightarrow s') &= \log P_B(s | s') + \text{LSE}(\log F(s' \rightarrow \cdot)) \\ &= \log P_B(s | s') + \log \sum_{s'' \rightarrow s'} F(s' \rightarrow s'') \\ &= \log P_B(s | s') + \log F(s'), \end{aligned} \quad (14)$$

which can also be obtained from (12). The equation on the optimal policy $\pi_1^*(\cdot | s) = \text{Softmax}(Q_1^*(\cdot | s))$ transforms into

$$P_F(s' | s) = \exp(\log F(s \rightarrow s') - \text{LSE}(\log F(s \rightarrow \cdot))) = \exp(\log F(s \rightarrow s') - \log F(s)), \quad (15)$$

which also coincides with the equation on P_F from (12).

If we try to look into the algorithm described in Section 3 in terms of flow functions, one can interpret that it applies MCTS on top of a neural network $\log F_\theta(s \rightarrow s')$ and tries to estimate $\log F_{\text{tree}}(s \rightarrow s')$ for edges in the tree. The update formula (7) actually coincides with (14):

$$\log F_{\text{tree}}(s \rightarrow s') = \log P_B(s | s') + \text{LSE}(\log F_{\text{tree}}(s' \rightarrow \cdot)). \quad (16)$$

B. Experimental Details

We utilize PyTorch (Paszke et al., 2019), and our implementations are based upon the published code of (Tiapkin et al., 2024). We implement MENTS in C++ for better performance.

B.1. Hypergrid

The reward at a terminal state s with coordinates (s^1, \dots, s^D) is defined as

$$R(s) = 10^{-3} + 0.5 \cdot \prod_{i=1}^D \mathbb{I} \left[0.25 < \left| \frac{s^i}{H-1} - 0.5 \right| \right] + 2 \cdot \prod_{i=1}^D \mathbb{I} \left[0.3 < \left| \frac{s^i}{H-1} - 0.5 \right| < 0.4 \right].$$

We use similar hyperparameters to previous works (Bengio et al., 2021; Malkin et al., 2022; Madan et al., 2023; Tiapkin et al., 2024). All models are parameterized by MLP with 2 hidden layers and 256 hidden units. We use Adam optimizer with a learning rate of 10^{-3} and a batch size of 16 trajectories. We take SubTB hyperparameter $\lambda = 0.9$. The difference from (Tiapkin et al., 2024) is that for SoftDQN, we do not use a replay buffer and use MSE loss instead of Huber. We use hard updates for the target network (Mnih et al., 2015) with a frequency of 3 iterations. For MENTS we take $\varepsilon = 0.01$. We perform hypergrid experiments on CPUs.

In Table 1, we measure the runtime of the algorithms during training and inference. As expected, the speed of MENTS decreases with the increase of the number of rounds due to additional Q_θ evaluations. However, we note that training with MENTS (4 rounds) runs faster than with SubTB and has better convergence than both SubTB and vanilla SoftDQN (see Figure 1).

Table 1. Training and inference speed on hypergrid environment measured on Apple M1 CPU. One iteration coincides with a batch of 16 trajectories in all cases. The lower training speed of `SubTB` in comparison to `SoftDQN` is due to the fact that the number of terms in its loss is quadratic in the trajectory length.

Method	Training	Inference
SubTB	8.5 it/s	35.6 it/s
SoftDQN	20.5 it/s	35.8 it/s
SoftDQN + MENTS 4	12.3 it/s	14.0 it/s
SoftDQN + MENTS 8	8.1 it/s	9.2 it/s
SoftDQN + MENTS 16	5.3 it/s	6.3 it/s

B.2. Bit Sequences

The set of modes M is constructed as defined in (Malkin et al., 2022), and we use the same size $|M| = 60$. Take $H = \{ '00000000', '11111111', '11110000', '00001111', '00111100' \}$. Then, each sequence in M is constructed by randomly taking $n/8$ elements from H with replacement and concatenating them. The test set for computing reward correlations is constructed by taking a mode and flipping i random bits in it, which is done for each mode and each $0 \leq i < n$.

We use the same Monte Carlo estimate for P_θ as in (Tiapkin et al., 2024):

$$P_\theta(x) = \mathbb{E}_{P_B(\tau|x)} \frac{P_F(\tau|\theta)}{P_B(\tau|x)} \approx \frac{1}{N} \sum_{i=1}^N \frac{P_F(\tau^i|\theta)}{P_B(\tau^i|x)}, \quad \tau^i \sim P_B(\tau|x).$$

All models are parameterized by Transformer (Vaswani et al., 2017) with 2 hidden layers, 8 attention heads and 64 hidden dimension. We use Adam optimizer with a learning rate of 10^{-3} and a batch size of 16. For `SubTB` we tune λ from $\{0.9, 1.1, 1.9\}$. For training `SoftDQN`, we use hard updates for the target network with a frequency of 5 iterations and use Huber loss following (Tiapkin et al., 2024). We also utilize a prioritized replay buffer (Schaul et al., 2016) with the same hyperparameters as in (Tiapkin et al., 2024). For `MENTS` we take $\varepsilon = 0.001$. We use NVIDIA A100 GPUs for bit sequence experiments.

In this case the runtime cost of tree manipulation in MCTS is dominated by the cost of Q_θ forward passes, thus the inference speed decreases proportionally to the number of MCTS rounds.